Landslide faults and tectonic faults, analogs?: The Slumgullion earthflow, Colorado

Joan Gomberg   U.S. Geological Survey, Center for Earthquake Research and Information, University of Memphis, Memphis, Tennessee 38152
Paul Bodin   Center for Earthquake Research and Information, University of Memphis, Memphis, Tennessee 38152
William Savage   U.S. Geological Survey, MS 966, Box 25046, Denver Federal Center, Denver, Colorado 80225
Michael E. Jackson   Cooperative Institute for Research in Environmental Sciences, University of Colorado, Boulder, Colorado 80309

ABSTRACT

Recent geophysical observations of landslide movement support the hypothesis that processes involved in landslide faulting are analogous to those that operate in crustal-scale faulting. Relative to crustal faulting studies, quantitative seismic, geodetic, and creep measurements of landslide deformation may be made in a very short time with readily available instrumentation and at relatively minimal expense. Our results indicate that the displacement of landslide material occurs along discrete faults exhibiting a combination of brittle failure, indicated by slide quakes and creep events, and as stable sliding observed as steady-state creep. Although slide quakes were observed, a more steady-state failure process of relieving accumulating strain is indicated.

INTRODUCTION

It has been noted that landforms observed on certain types of landslides are strikingly similar to those associated with crustal-scale faults (Fig. 1) (Fleming and Johnson, 1989). This superficial similarity suggests the hypothesis that some landslides may provide useful analogs for the study of processes involved in crustal-scale tectonics, thus bridging the gap between laboratory experiments and regional field studies. We present observations of geomorphic and geophysical expressions of landslide faulting that support this hypothesis. The benefits of landslides as models are evident in the fact that much of the data we present were collected within a week by using conventional geophysical instrumentation from an area spanning <0.5 km^2. Our results, in addition to demonstrating further the analogous behavior of landslides and crustal faulting, suggest several new opportunities for monitoring and evaluating landslide deformation and the hazards that landslides pose.

Our experiment was designed to observe indicators of slide rheology and modes of deformation. In particular, we hoped to determine (1) if the displacement of landslide material occurs primarily along faults bounding the landslide (Crandell and Varnes, 1961) or along distributed shear zones; (2) whether landslide fault slip takes place seismically or as aseismic fault creep; (3) if slide quakes can be observed (indicating brittle failure); and (4) how the rate and distribution of seismicity and creep correlate with the rate of fault slip.

To address these questions we deployed and operated a buried digital high-precision creepmeter and a portable seismic network in the vicinity of one of the major strike-slip faults bounding the Slumgullion landslide in southwestern Colorado (Fig. 2). We conducted our field study during June 22–28, 1993. Relative velocity vectors were also measured by using the Global Positioning System (GPS) methods. Additional measurements made over several months included creep observations from a modified analog tide gauge and the displacement field evident in a grid of stakes. Both sets of measurements were made in the same region covered by the seismic network (Fig. 3). Our
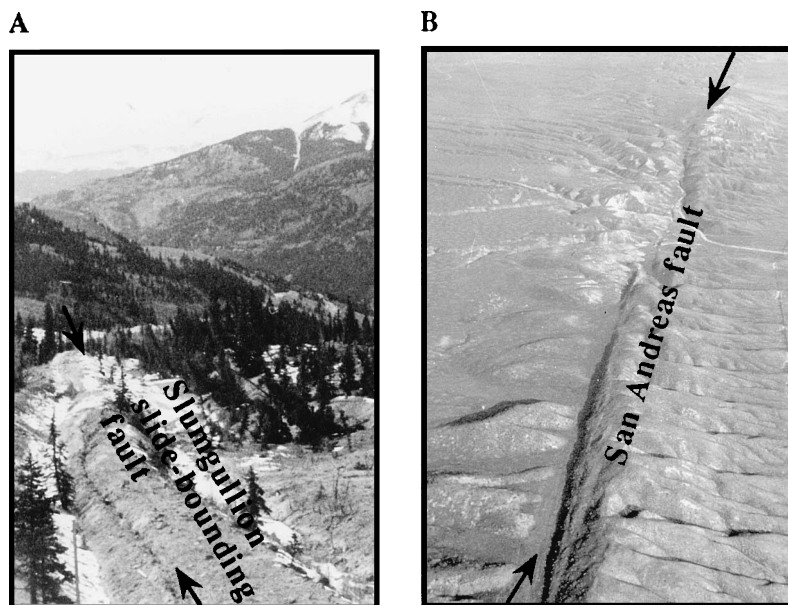

Figure 1. A: View looking along trend (indicated by arrows) of slide-bounding strike-slip fault on Slumgullion landslide in Colorado. B: View along trend of strike-slip San Andreas fault in Carizzo Plains of California (photo by R. E. Wallace, 1990, U.S. Geological Survey). Similarity between adjacent ridges parallel to San Andreas and Slumgullion faults suggests that such structures are common to strike-slip faults of all scales. Their absence along many crustal faults may be attributed to higher erosion rates relative to crustal fault slip rates.
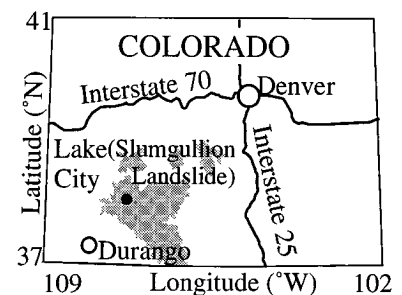

Figure 2. Map of Colorado and site of Slumgullion landslide near Lake City. Shading indicates distribution of Tertiary volcanic rocks of San Juan Mountains. Interstate highways 70 and 25 are shown for reference.
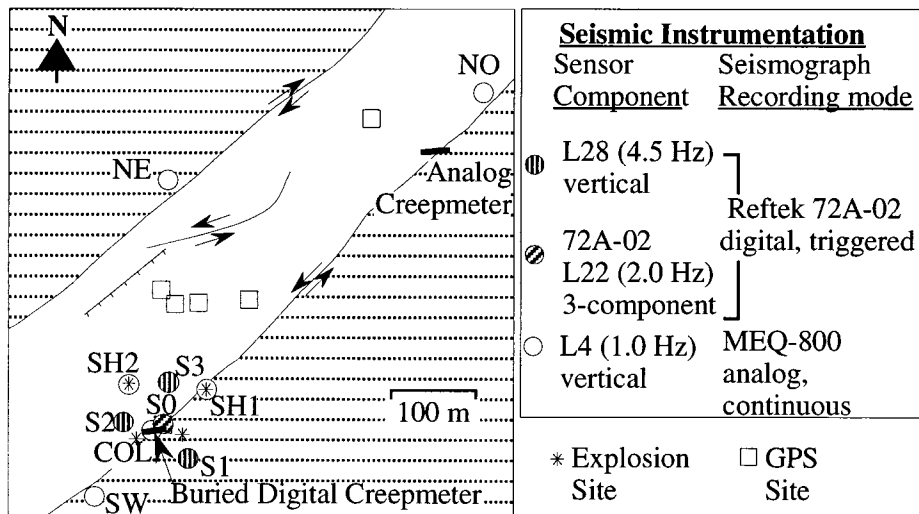
Figure 3. Schematic map of Slumgullion landslide, our seismic network (station codes labeled), creepmeters, and Global Positioning System (GPS) observation points (points on headscarp and toe are not shown). These instruments were located to monitor one of major slide-bounding strike-slip faults where displacement rate of slide mass is greatest (~16 mm/d). Major mapped faults within and/or bounding slide (diagonal-rule pattern—normal faults; solid line with arrows—strike-slip fault). Four explosions (asterisks) were made and recorded to determine velocity structure. Head scarp is above top of figure.
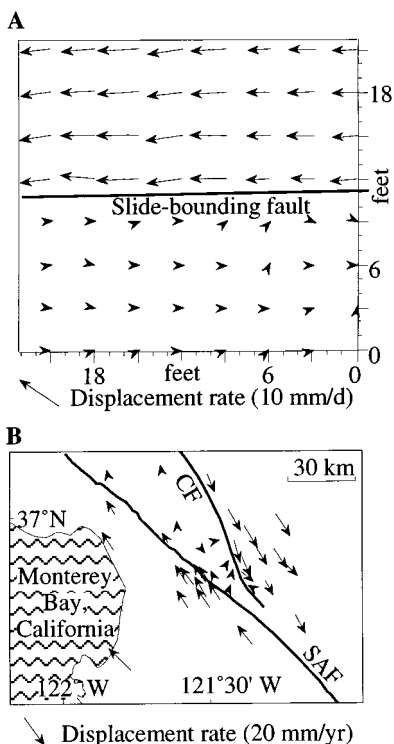

Figure 4. A: Displacement vectors (relative to point at 0, 0) measured during May 19 to June 29, 1993, for grid of stakes spanning slide-bounding strike-slip fault of Slumgullion landslide. Grid was located several metres up landslide from digital creepmeter (see Fig. 3). B: Velocity vectors inferred from geodetic networks spanning creeping segments of San Andreas (SAF) and Calavaras (CF) faults (from Fig. 6 of Lisowski et al., 1991). Velocities indicate motion relative to network "center of mass" (Lisowski et al., 1991).

most rapidly moving central region of the slide, and 4 mm/d in the toe region, consistent with average rates determined during the past 30 yr by surveying and by photogrammetric analyses (Fig. 5; Crandell and Varnes, 1961; Smith, 1993). This similarity and the benefits of GPS surveying—i.e., not needing line of sight between observation points as well as the ability to obtain measurements fixed in an absolute reference frame—suggest that GPS surveying has a promising future in landslide deformation monitoring and hazard assessment.

SEISMIC OBSERVATIONS

Results of analyses of portable seismic network data suggest that slide quakes exist and are detectable with conventional instrumentation. Slide quakes are observed as short-duration, spatially and temporally clustered signals (Fig. 6A); the sources are probably from the slide-bounding strike-slip faults (Fig. 7). The seismic network that recorded these slide quakes included four analog seismographs and a phased digital microarray. The analog seismographs operated with single-component sensors. Their internal clocks were synchronized daily to radio-broadcasted time and had drift rates that were insignificant relative to the precision with which seismic phases could be timed. A phased digital microarray, located inside the analog network and crossing the slide-bounding fault, contained three single-component sensors spaced at 50 m from a central three-component set of sensors (Fig. 3). The digital signals were recorded on a single seismograph synchronized continuously to radio-broadcasted time. The relative arrival times at each station for 13 of the most well-recorded slide quakes show that they originated in essentially the same location. This enabled us to treat them as one event with little loss of information, and to use the average relative arrival times to determine the event's location (hypocenter). The nonimpulsive onsets and slightly dispersed wave trains of these signals and ray-tracing analyses indicated that
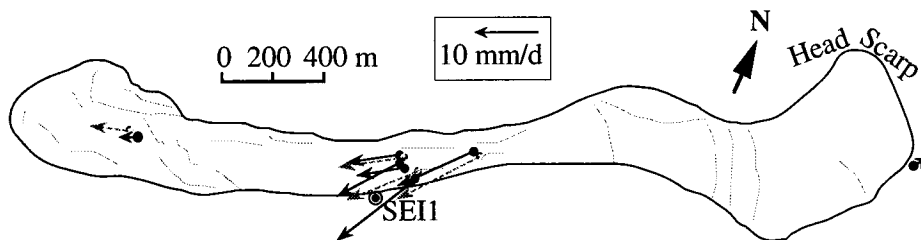
analyses also benefited from the work of others who have studied the deformation of the Slumgullion during the past 35 years (e.g., Crandell and Varnes, 1961).

GEODETIC OBSERVATIONS

The displacement of the stake grid shows that deformation in the immediate vicinity of the slide-bounding strike-slip fault occurs as block motion (Fig. 4). Essentially rigid block motion is also observed across creeping segments of crustal strike-slip faults, the San Andreas and Calavaras faults, which accommodate plate motions principally by continuous creep (Fig. 4; Savage and Burford, 1971; Lisowski et al., 1991).

Satellite geodesy measurements confirm that the deformation of the landslide inferred from our experiment was representative of the long-term average. During a 100 h period in June 1993, GPS-determined displacement rates were 12–15 mm/d in the

Figure 5. Velocity vectors, relative to site SEI1, measured by using GPS (solid lines with arrows) and vectors measured by surveying and by photogrammetric methods (shaded lines with arrows); differences are within probable measurement errors. Active part of slide is outlined; nonzero value (2–3 mm during survey period) just above head-scarp is probably due to monument instability.
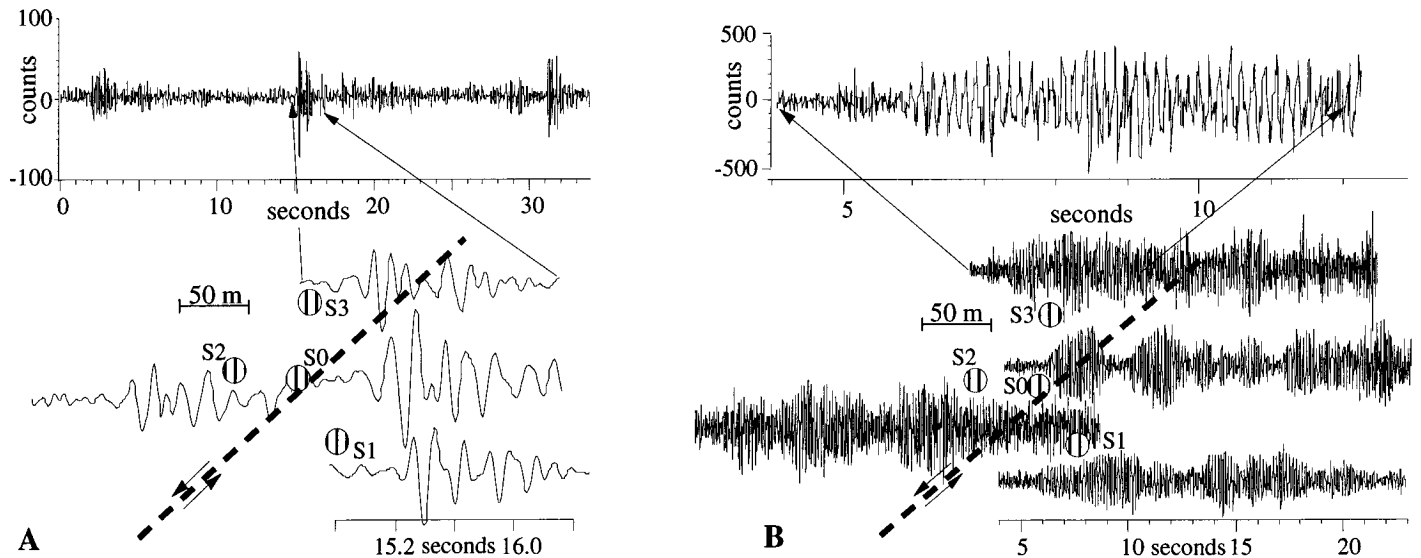
Figure 6. Ground motions recorded on Slumgullion landslide. All traces shown were recorded by digital microarray and are plotted on same amplitude and time scales. Only vertical-component seismograms are shown; each was recorded by sensor denoted by nearest corresponding striped circle. Top trace spans longer duration and includes segment shown from sensor S3. A: Seismograms of probable slide quakes. B: Sinusoidal seismograms.

the observed signals were surface waves (Figs. 6A and 7). Hypocenter estimation requires knowledge of the seismic velocity structure. Arrival times measured for P and S waves on seismograms of four explosions guided trial-and-error ray tracing to determine the velocity structure. The resultant P and S wave velocities indicate that the Poisson's ratio within the slide is ~0.49. Such a high value is consistent with models of slide deformation in which the slide material behaves plastically on some time scales (Savage and Smith, 1986).

Long-duration, sinusoidal signals were also observed (Fig. 6B). These signals may originate from slide-generated sources, but their generation by nonnatural sources such as vehicle traffic cannot be ruled out. The emergent onset of these signals makes timing of their arrival and estimating their hypocenters extremely difficult. Although they were observed most commonly at stations closest to the traffic, in several instances the most distant stations recorded the largest amplitudes. The frequency of occurrence of these signals and the time of day did not correlate clearly; thus, their association with traffic was ambiguous (nighttime traffic was minimal). We suggest that several sources may give rise to these monochromatic signals, some natural and others artificially generated. Possible natural sources include slow rupture of faults or materials entrained within the faults (e.g., trees, boulders), or slow basal slip along the landslide-bedrock interface.

CREEP OBSERVATIONS

The analog long-term creepmeter observations are consistent with seasonal variations around a steady rate of ~15 mm/d. We note that the creeping section of the San Andreas fault also exhibits seasonal variations (Fig. 8A). It is unlikely that the physical laws governing or the forces driving de-
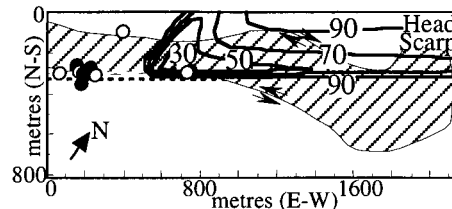
Figure 7. Map of probable epicentral locations of slide quakes observed during experiment. Contoured values are confidence levels (in percent probability) that contour encloses epicenter; regions with highest probabilities are enclosed by contours with smallest numbers. Probabilities are calculated by using grid-search algorithm (Tarantola and Valette, 1982; Gomberg et al., 1989) that assumes: (1) velocity structure varies only laterally and (2) observed signals are surface waves traveling along straight-line trajectories between source and seismic station. Shear (or group) velocity north of dashed line is 0.286 km/s, and south of line it is 3.600 km/s. Circles indicate seismic stations (open-analog, solid-digital); striped region delineates active slide. Validity of model and algorithm was verified by using them to estimate epicenters of four explosions. Estimated explosion locations were within 30 m of true locations. Results are insensitive to reasonable changes in model velocities.

formation for either the San Andreas fault or the Slumgullion earthflow vary seasonally. This leaves variations in the fault rheology, perhaps due to seasonal pore-pressure variations, as the common cause of
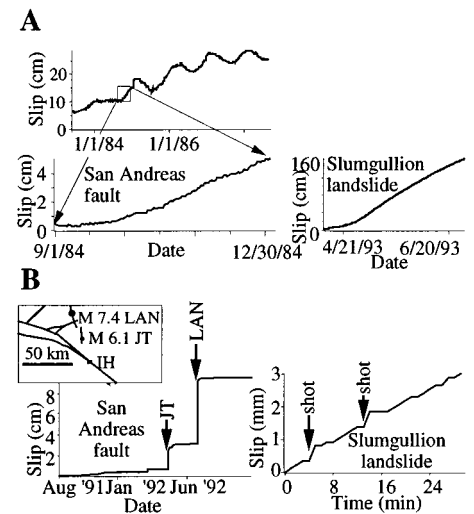
Figure 8. Creep measured across San Andreas fault (left) and slide-bounding strike-slip fault on Slumgullion landslide (right; W. Savage and R. W. Fleming, unpublished). A: Change in slope in both cases probably is due to increased climatic moisture, i.e., spring rains along San Andreas fault and spring snow melt on Slumgullion landslide. B: Creep events induced by Joshua Tree (JT) and Landers (LAN) earthquakes near San Andreas fault measured at Indio Hills (IH) creepmeter (data and map inset on left) and by explosions (shots) near Slumgullion landslide (right).

seasonal slip-rate variations. Moreover, we recorded creep events triggered by explosions that were set off several tens of metres from the fault (to calibrate the velocity structure for the seismic data analysis) (Fig. 8B). It was not possible to assess whether these triggered creep events were seismogenic, because their signals would be obscured by those generated by the explosions. Creep events triggered by earthquakes have been documented along the San Andreas fault but are not well understood (Bodin et al., 1994). The observation that creep events can actually be created along the landslide fault suggests that controlled experiments of triggered creep could be done in the future. The observations of slide quake signals and of triggered creep events imply that, at least on short time scales, the landslide material behaves elastically, storing and releasing elastic strain energy.

DISCUSSION

Although our measurements spanned only a short time on a single landslide, our results suggest that landslide deformation that occurs along the slide-bounding fault is most analogous to creeping crustal faults. We draw an analogy to the San Andreas fault zone because it is the only fault in which both creep and seismicity are well documented. A segment of the San Andreas fault zone in central California creeps at the fault's long-term slip rate (Savage and Burford, 1971), indicating that steady-state slip almost completely relieves accumulating strain. In addition to a nearly constant slip rate, this creeping section of the San Andreas also exhibits a high rate of small-magnitude seismicity. The relation between the production of small earthquakes and creep is not well understood. Our observations of creep and seismicity, probably associated with slip along the landslide's strike-slip fault, suggest that similar processes may be operating on both the Slumgullion and San Andreas faults. The accessibility (in three dimensions) and the potential to do controlled experiments (e.g., create creep or seismic events) along the landslide fault make it an ideal natural laboratory for the study of crustal faults. We note that moderate earthquakes have ruptured through creeping sections of the San Andreas fault, and we cannot dismiss the possibility that larger slide quakes may also occur and/or that other sections of the landslide fault may exhibit different behaviors.

Slide quakes may occur more frequently than our observations indicate because the small amplitudes of the slide quake signals were only discernible during periods of low background noise levels. Observed amplitudes of the slide quake signals provide an estimated source-rupture dimension of ~ 230 m^2. The local magnitude of an event with amplitudes just above the noise on the analog recorders is $m_L \sim 0$. This corresponds to a scalar seismic moment of $M_o \sim 10^9$ N $\cdot$ m (Thatcher and Hanks, 1973). The scalar seismic moment is

$$M_o = \mu u A, \tag{1}$$

where μ = rigidity, u = average slip, and A = rupture area. The average slip may be estimated from the shear stress,

$$\tau \approx \mu(u/D), \tag{2}$$

in which D is the width of the rupture area. Letting L = rupture length, the spatial dimensions of the rupture can be related to the moment and shear stress as

$$D^2 L = M_o/\tau. \tag{3}$$

The Coulomb equation and measurements made on the Slumgullion landslide restrict τ. The former is

$$\tau = \tau_c + \sigma_n \tan \phi, \tag{4}$$

in which τ_c (yield strength or cohesive shear strength) = 0.25–0.54 MPa, σ_n (normal or lithostatic stress) = $\rho g h$ = 0.1 MPa, ρ (density) = 1500 kg/m^3, g (acceleration of gravity) = 9.8 m/s^2, h (half the average depth of the active slide) = 13/2 m, and ϕ (angle of internal friction) = 10° (Parise and Guzzi, 1991). This yields $D^2 L \sim 3 \times 10^9$ cm^3. If we require $D \sim 2h = 13$ m, $L \sim 18$ m and the rupture area is ~ 230 m^2.

CONCLUSIONS

We have demonstrated that quantitative measures of landslide deformation (seismic, geodetic, and creep observations) can be made in a short time with readily available instrumentation. The analogous nature of these observations to those recorded near crustal faults with more complex instrumentation deployed for much longer time periods suggests that much could be learned from future studies of landslide faulting. Our results also illustrate two new potential approaches to evaluating landslide deformation and hazard: (1) the use of GPS technology to map the surface-velocity field and (2) seismic monitoring of slide quake activity.

The displacement of landslide material appears to occur along discrete faults exhibiting a combination of brittle failure, evidenced by slide quakes and creep events, and stable sliding, evidenced by steady-state creep. Although slide quakes were observed, a more steady-state failure process of relieving accumulating strain is indicated. The manner in which the rate and distribution of seismicity and creep correlate with fault-slip rate remains to be determined in future experiments.

REFERENCES CITED

Bodin, P., Bilham, R., Behr, J., Gomberg, J., and Hudnut, K. W., 1994, Slip triggered on southern California faults by the Landers earthquake sequence: Seismological Society of America Bulletin, v. 84, p. 806–816.

Crandell, D. R., and Varnes, D. J., 1961, Movement of the Slumgullion earthflow near Lake City, Colorado, *in* Short papers in the geologic and hydrologic sciences: U.S. Geological Survey Professional Paper 424-B, p. 136–139.

Fleming, R. W., and Johnson, A. M., 1989, Structures associated with strike-slip faults that bound landslide elements: Engineering Geology, v. 27, p. 39–114.

Gomberg, J., Shedlock, K., and Roecker, S., 1989, The effect of S wave arrival times on the accuracy of hypocenter estimation: Seismological Society of America Bulletin, v. 80, p. 1605–1628.

Lisowski, M., Savage, J. C., and Prescott, W. H., 1991, The velocity field along the San Andreas fault in central and southern California: Journal of Geophysical Research, v. 96, p. 8369–8391.

Parise, M., and Guzzi, R., 1991, Volume and shape of the active and inactive parts of the Slumgullion landslide, Hinsdale County, Colorado: U.S. Geological Survey Open-File Report 92-216, 29 p.

Savage, J. C., and Burford, R. O., 1971, Strain accumulation along the San Andreas fault: Discussion: Journal of Geophysical Research, v. 76, p. 6469–6479.

Savage, W. Z., and Smith, W. K., 1986, A model for the plastic flow of landslides: U.S. Geological Survey Professional Paper 138S, 32 p.

Smith, W. K., 1993, Photogrammetric determination of movement on the Slumgullion slide, Hinsdale County, Colorado, 1985–1990: U.S. Geological Survey Open-File Report 93-597, 17 p.

Tarantola, A., and Valette, B., 1982, Inverse problems = Quest for information: Journal of Geophysics, v. 50, p. 159–170.

Thatcher, W., and Hanks, T. C., 1973, Source parameters of southern California earthquakes: Journal of Geophysical Research, v. 78, p. 8547–8576.